

General Disclaimer

One or more of the Following Statements may affect this Document

- This document has been reproduced from the best copy furnished by the organizational source. It is being released in the interest of making available as much information as possible.
- This document may contain data, which exceeds the sheet parameters. It was furnished in this condition by the organizational source and is the best copy available.
- This document may contain tone-on-tone or color graphs, charts and/or pictures, which have been reproduced in black and white.
- This document is paginated as submitted by the original source.
- Portions of this document are not fully legible due to the historical nature of some of the material. However, it is the best reproduction available from the original submission.

(NASA-CF-143438) THE PROPAGATION OF PLANE
WAVES AND HIGHER ORDER ACOUSTIC MODES IN
MULTISECTIONED DUCTS (Pennsylvania State
Univ.) 14 p HC \$3.25

CSCL 204

N75-31856

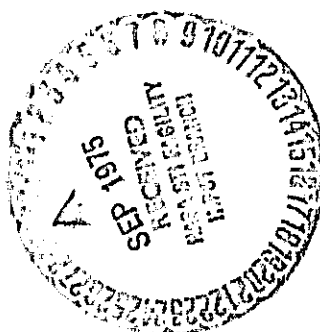
Unclass
G3/71 35263

THE PROPAGATION OF PLANE WAVES AND HIGHER ORDER
ACOUSTIC MODES IN MULTISECTIONED DUCTS

by

B.R. Wyerman and G. Reethof

The Pennsylvania State University
University Park, Pennsylvania 16802



Grant No. NGL 39-009-121

Date: September 25, 1975

THE PROPAGATION OF PLANE WAVES AND HIGHER ORDER
ACOUSTIC MODES IN MULTISECTIONED DUCTS

by

B.R. Wyerman and G. Reethof

The Pennsylvania State University
University Park, Pennsylvania 16802

Summary

A theoretical and experimental study of acoustic propagation in an anechoically terminated multisectioned duct has been performed. A unique source array consisting of two concentric rings of sources, providing phase and amplitude control in the radial as well as circumferential direction, was developed to generate plane waves and both spinning and non-spinning higher order modes. Measurement of attenuation and radial mode shapes were taken with finite length liners inserted between the hard wall sections of a duct with an anechoic termination. Materials tested as liners included fiberglass and both perforated sheet metals and feltmetals with a honeycomb backing. A search technique has been developed to find the complex eigenvalues for a liner under the assumption of a locally reacting boundary condition. The experimental results were compared with a theoretical analysis which includes the modal transmission and reflection at the interface of each duct section. The comparison indicates that the local reaction boundary condition is valid for these three liner configurations. The results of this study suggest that better liner performance may be obtained by extending theoretical and experimental work to explore segmented duct configurations made up of a combination of several different liner materials.

Introduction

The propagation of plane waves and higher order acoustic modes in lined and unlined ducts has been a subject of continued interest. Most studies, however, have been limited to modal transmission and lining design for infinite ducts. Recent investigations have shown that acoustic propagation through a multisectioned duct may produce attenuation in excess of that for continuously lined ducts (1, 2). The majority of this analysis has been restricted to theoretical considerations with little experimental data to substantiate the stated results. Therefore, the purpose of this study was to verify current multisectioned duct theory and to investigate the boundary conditions and attenuation properties for various liner materials using analytical and

experimental approaches.

Experimental Apparatus

The multisectioned duct used in this experiment is shown in Figure 1. The duct itself is made of 12 inch diameter transite pipe. Despite the fact that no flow was considered, the section in front of the liner coupled to the source array will be called the upstream section and the section behind the liner coupled to the anechoic termination will be called the downstream section. The test section is a 14 inch diameter transite pipe which will accomodate one inch thick liners with no change in cross sectional area throughout the duct. A half inch diameter condenser microphone with a 4 mm. probe tube was used to measure radial mode shapes at the stations indicated in Figure 1.

The source array shown in Figure 2 contained thirteen 2-1/4 inch diameter loudspeakers placed in an aluminum plate. Eight speakers were placed in an outer ring near the radius of the duct, four speakers within a smaller ring, and one speaker at the center of the duct. The positions of the speakers were chosen to insure that the desired modes would be generated with maximum efficiency. Obviously, the speaker at the center could only be used in generating non-spinning ($m = 0$) modes. The cut-off frequencies for the various modes generated are shown in Figure 3. By individually controlling the phase and amplitude of each element in the array, both spinning and non-spinning modes could be generated within the duct at and above their cut-off frequencies.

Five materials were chosen for duct liners. These included two perforated sheet metals of 30% and 22.5% open area, two feltmetals with flow resistances of 45 and 25 cgs rayls, and a fiberglass material. The fiberglass was a one inch thick commercially available material used for pipe insulation. Both the feltmetals and perforated metals were tested with a 7/8 inch deep closed cell honeycomb core cavity behind the material. No attempt was made to optimize the impedance parameters of our liners by altering cavity depth or material parameters. Instead, it was decided to choose materials that could be inserted within the one inch depth provided by our test section. In later figures, the following abbreviations for each material will be used.

1. FM 1 - Feltmetal, 45 cgs rayls
2. FM 2 - Feltmetal, 25 cgs rayls
3. Perf 1 - Perforate, 22.5% open area
4. Perf 2 - Perforate, 30% open area
5. Fiberglass - one inch thick fiberglass

Theory

Zorumski's multisectioned duct theory (1) has been generalized to consider the case of an anechoically terminated hollow duct of three sections with no flow. This corresponds to our experimental configuration shown in Figure 1. Furthermore, the source distribution has been modified to account for our 13 element speaker array. This theory considers the modal transmission and reflection at the interface of each duct section as determined by the boundary conditions and eigenvalues. In Figure 4, the modal amplitudes $A_{m\mu\nu}^{+j}$ at each interface are related to the transmission coefficients $T_{m\mu\nu}^{+j+k}$ and reflection coefficients $R_{m\mu\nu}^{+j+k}$ in the following manner (1).

$$\{A_{m\mu\nu}^{+2}\} = [T_{m\mu\nu}^{+2} \quad +_1] \{A_{m\mu\nu}^{+1}\}$$

$$\{A_{m\mu\nu}^{+3}\} = [R_{m\mu\nu}^{+3} \quad -_3] \{A_{m\mu\nu}^{-3}\} + [T_{m\mu\nu}^{-3} \quad +_3 \quad +_2] \{A_{m\mu\nu}^{+2}\}$$

$$\{A_{m\mu\nu}^{-1}\} = [T_{m\mu\nu}^{-1} \quad -_2] \{A_{m\mu\nu}^{-2}\}$$

$$\{A_{m\mu\nu}^{-2}\} = [R_{m\mu\nu}^{-2} \quad +_2] \{A_{m\mu\nu}^{+2}\} + [T_{m\mu\nu}^{-2} \quad -_3] \{A_{m\mu\nu}^{-3}\}$$

From this analysis, the modal amplitudes at the interface of each section can be calculated. The eigenvalues for the hard wall duct sections are the real zeroes of derivatives of the Bessel functions (3). Within the liner section, the complex eigenvalues are determined by the local reaction boundary condition using impedance contours for each material measured with a standing wave tube. The eigenvalue equation becomes

$$\beta i k a J_m(k_r a) - m J_m(k_r a) + k_r a J_{m+1}(k_r a) = 0$$

The eigenvalues are calculated by using the Principle of the Argument (4) and performing successive contour integrations in the complex plane. The integration contours shown in Figure 5 are expanded outward from the origin and the integration is performed in the clockwise direction. Once a contour is found where the eigenvalue exists, a first approximation is chosen and an iteration technique locates the exact eigenvalue. The correct order of these eigenvalues can be determined from examination since their real component is interlaced between the real zeros of the Bessel functions and their derivatives - the extreme cases for soft and hard walls respectively (5). The number of radial modes considered by the theoretical analysis has been limited to include

all cut-on modes at a given frequency within the hard wall section and the first two cut-off modes above that frequency.

Although modes were generated with each of the liners, the mode shapes for only one material will be presented - a 28-1/2 inch length of feltmetal, flow resistance 45 CGS rayls. In the following figures, the radial mode shapes measured at the duct stations in Figure 1 are shown when the array is shaded to generate the desired mode. The mode shapes at the two upstream locations show the incident wave and also the presence of a standing wave due to the impedance discontinuity of the liner. Within the liner, the mode shape changes somewhat since the eigenvalues are complex and differ from the eigenvalues for the hard wall section. In the downstream section, the mode shape again resorts to the form of the incident wave with noticeable contamination from other higher order radial modes. In cases where there is considerable attenuation due to the liner, the downstream mode shape often shows no relationship at all to the generated mode. This is because the mode is attenuated to such an extent after passing through the liner that residual components of plane waves and other modes are all that remain downstream. These residual modes are generated as the result of slight variations in the response of individual speakers in the source array. These variations generate additional modes of a different spin number together with the desired mode but at a much lower amplitude. If these modes can propagate at the particular frequency, they often appear downstream since they are not attenuated to the same extent by the liner as our desired mode. This result is noticeable particularly at high frequencies where several lower modes of a different spin number can also propagate. In addition, when the transmission loss across the liner is high, the major component of the propagating mode will be attenuated and an unrecognizable mode shape which is the combination of several residual modes results. Figure 6 shows radial mode shapes measured for the (0, 0) mode (plane wave) at 800 Hz. together with levels calculated from the theoretical analysis. Despite the presence of plane waves at upstream and downstream positions, a plane wave does not exist within the liner section. The mode shapes for the (0, 1) mode shown in Figure 7 exhibit a noticeable shift in the nulls that is predicted by theory. The first spinning mode (1, 1) is shown in Figure 8 as generated at 1000 Hz., well above the cut-off frequency. The benefits of providing radial, as well as circumferential, control of our array can be seen when generating higher order mode shapes. For the (1, 2) mode generated at 2700 Hz. and shown in Figure 10, the agreement with theory is considerably poorer than for the previous lower order modes. This is partly

because we are operating in a frequency range where several other modes can also propagate as can be seen in Figure 3. Mode shapes for the (0, 3) mode at 2535 Hz. are shown in Figure 10 for the two upstream locations. Downstream modes are eliminated due to the significant attenuation across the liner.

The transmission loss, the difference in power levels on each side of the liner, can be calculated from the modal amplitudes and is shown in Figures 11 through 14 for 28-1/2 inch lengths of each material in the presence of individual modes. It is interesting that the transmission loss for the (0, 1) mode decreases with frequency in contrast to the general behavior for the other modes. The low attenuation for this mode at high frequencies further complicates the problem of having residual modes. Since the (0, 1) mode is not readily attenuated by the liner at high frequencies, it is difficult to generate higher order mode shapes at frequencies where this mode can propagate.

Conclusions

It has been shown that the source array described previously can be used to advantage in generating higher order modes at and above their cut-off frequencies. Thus, having control of the radial as well as circumferential dependence of the elements in the array enhances the mode shapes considerably. In addition, the theoretical analysis and boundary condition adequately predicts the amplitudes and mode shapes at stations throughout the hard wall duct as well as in the liner. Best agreement with theory, however, occurred for modes that could propagate without contamination from other cut-on modes. The encouraging results of this study indicate that the multisected duct analysis could be extended to consider combinations of liners with impedance parameters chosen or designed in order to optimize their attenuation properties.

This work was conducted through support from NASA Langley Research Center under Grant No. NGL 39-009-121.

REFERENCES

1. Lansing, D.L. and Zorumski, W.F., "Effects of Wall Admittance Changes on Duct Transmission and Radiation of Sound", *J. Sound Vib.* 27, 85-100, 1973.
2. Zorumski, W.E., "Acoustic Theory of Axisymmetric Multisectioned Ducts", *NASA TR-R-419*, 1974.
3. Abramowitz, Milton and Stegun, Irene A., *Handbook of Mathematical Functions*, National Bureau of Standards, Washington, 1964, pp. 411-412.
4. Copson, E.T., *Theory of Functions of a Complex Variable*, Clarendon Press, Oxford, 1960, pp. 118-119.
5. Doak, P.E. and Vaidya P.G., "Attenuation of Plane Wave and Higher Order Mode Sound Propagation in Lined Ducts", *J. Sound Vib.*, 12, 201-224, 1970.

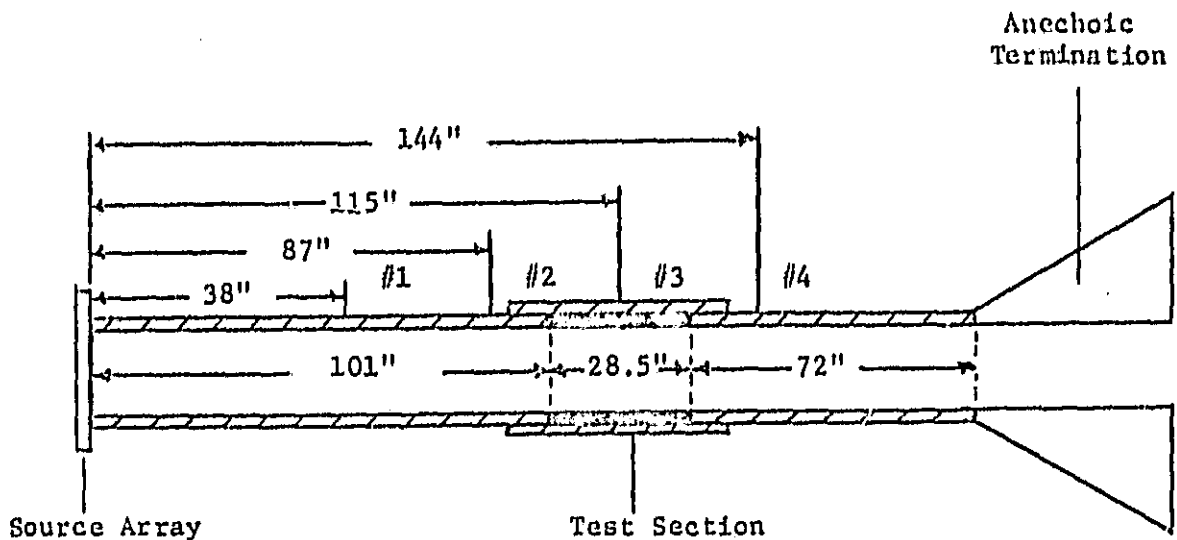


Figure 1
Experimental Duct Arrangement

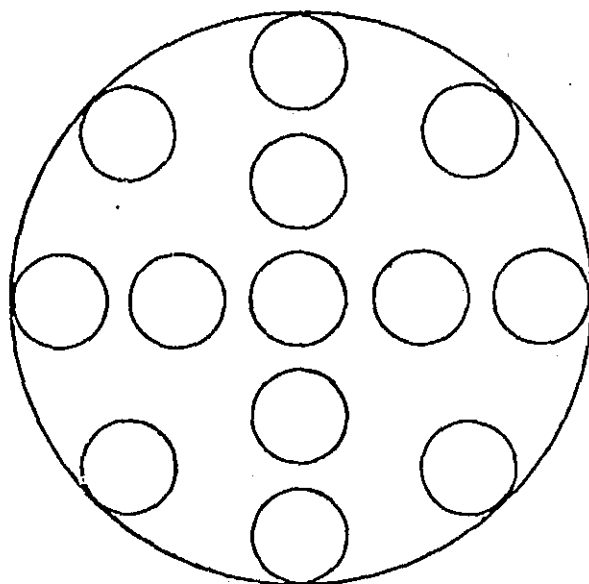


Figure 2
Source Array with Thirteen Elements

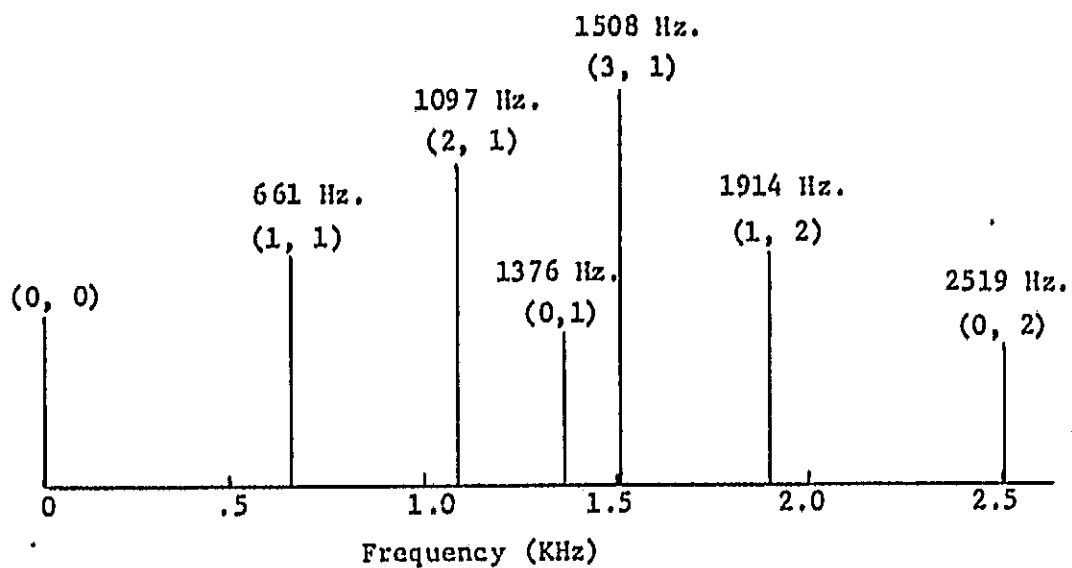


Figure 3
Cut-off Frequencies for Higher Order Modes

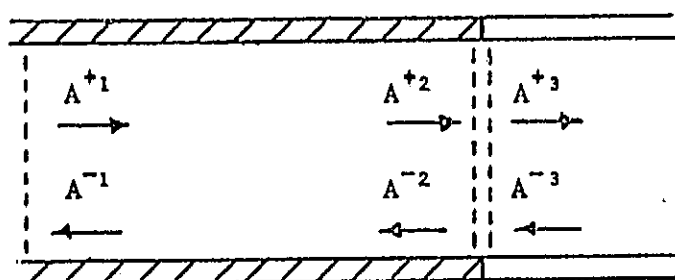


Figure 4
Modal Amplitudes at Interfaces for
Multisectioned Duct Analysis

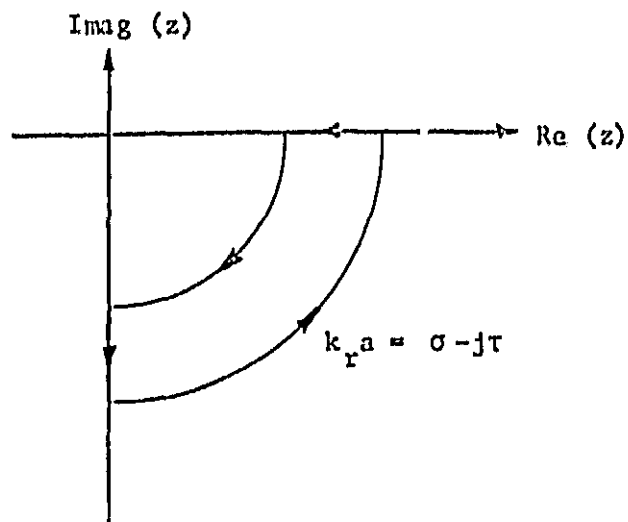


Figure 5
Integration Contour for Eigenvalue Search in Complex Plane

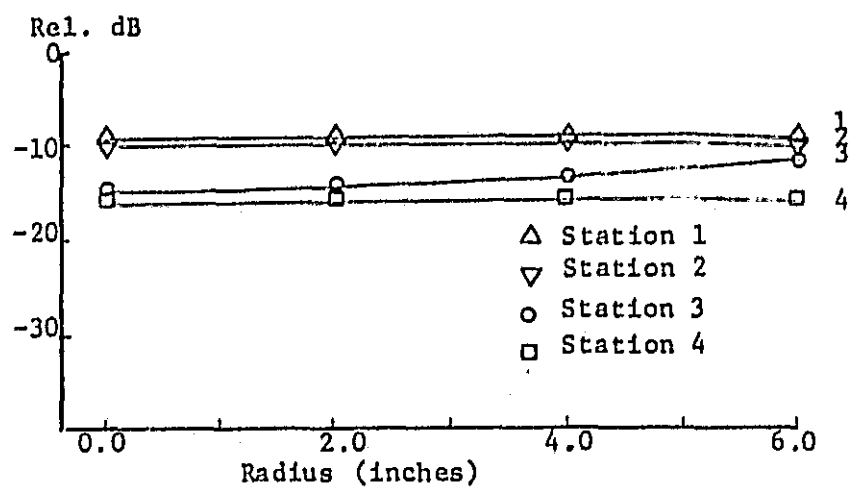


Figure 6
Modes Shapes for (0, 0) Mode,
800 Hz, - 28-1/2" FM 1 Liner

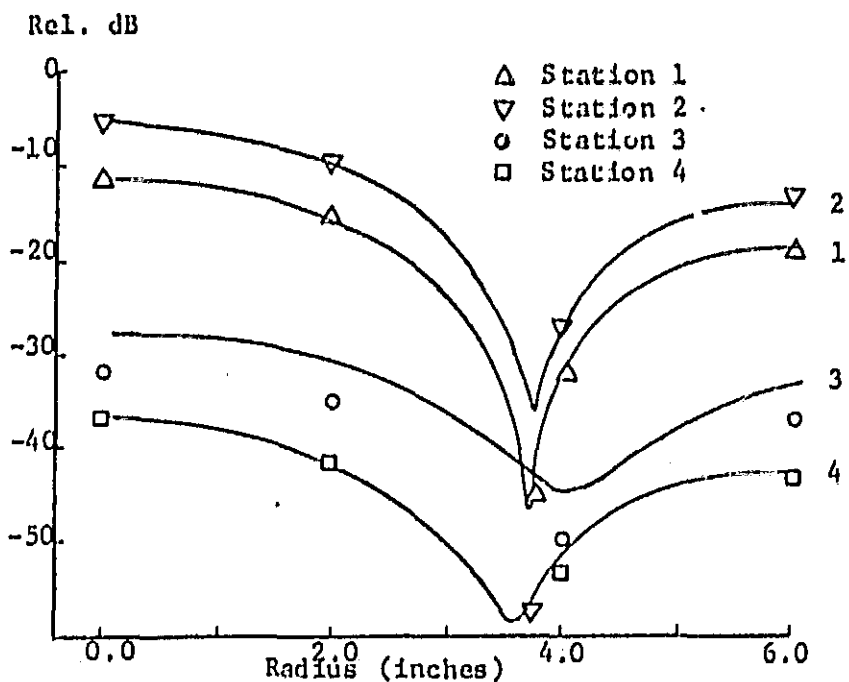


Figure 7
Mode Shapes for (0, 1) Mode,
1390 Hz. - 28-1/2" FM 1 Liner

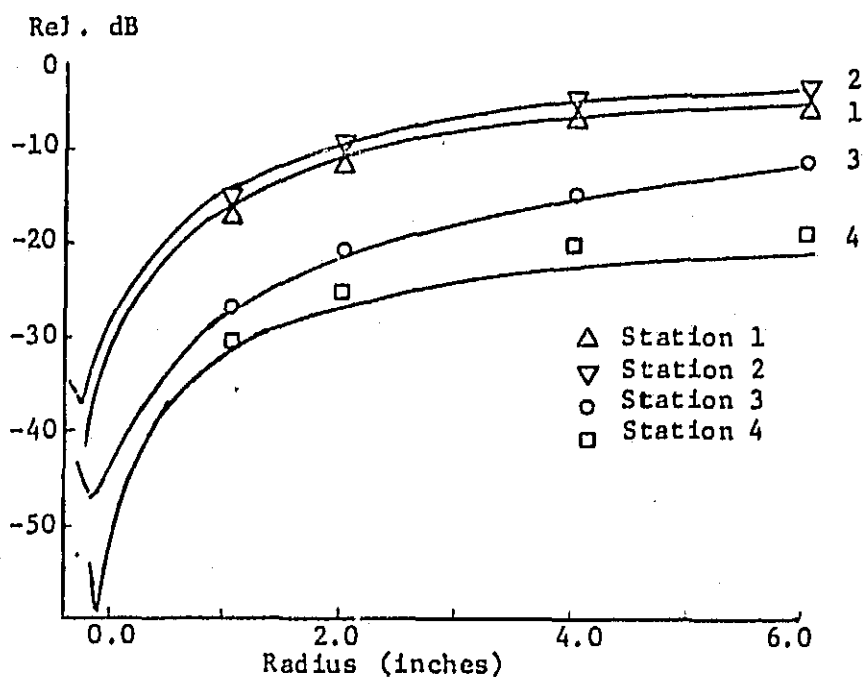


Figure 8
Mode Shapes for (1, 1) Mode,
1000 Hz. - 28-1/2" FM 1 Liner

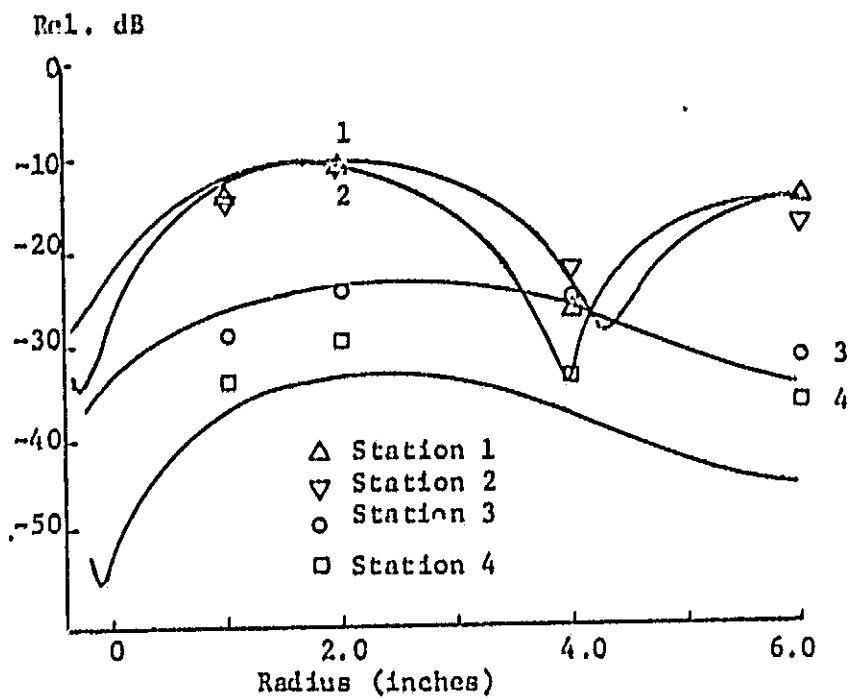


Figure 9
 Mode Shapes for (1, 2) Mode,
 2700 Hz. - 28-1/2" FM 1 Liner

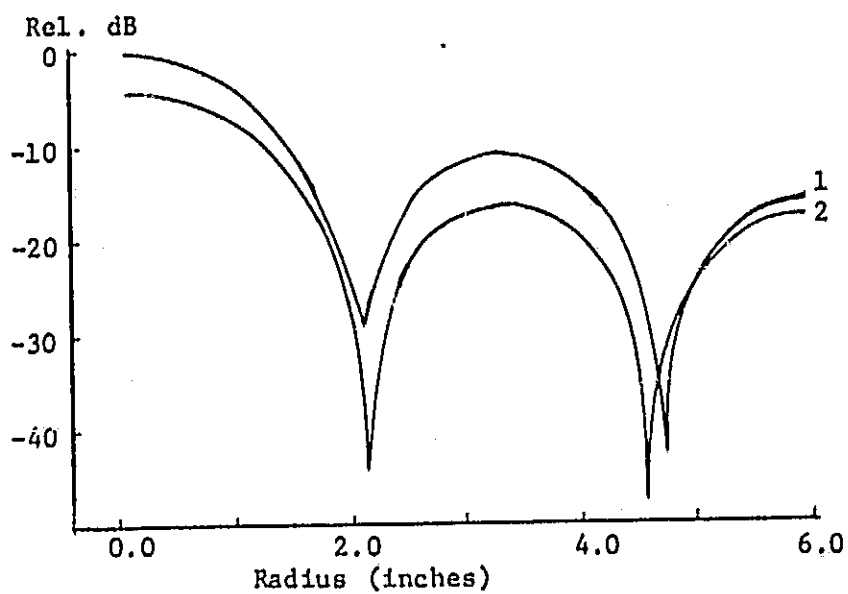


Figure 10
 Mode Shapes for (0, 2) Mode,
 2535 Hz. - Upstream Positions

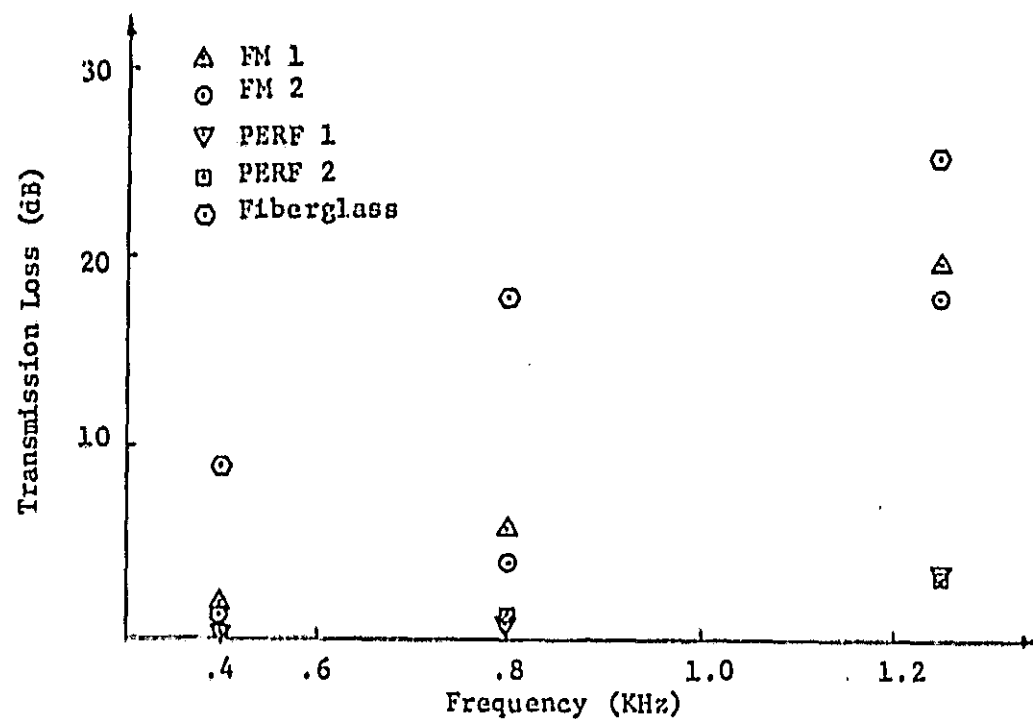


Figure 11
Transmission Loss for (0, 0)
Mode - 28-1/2" Liner

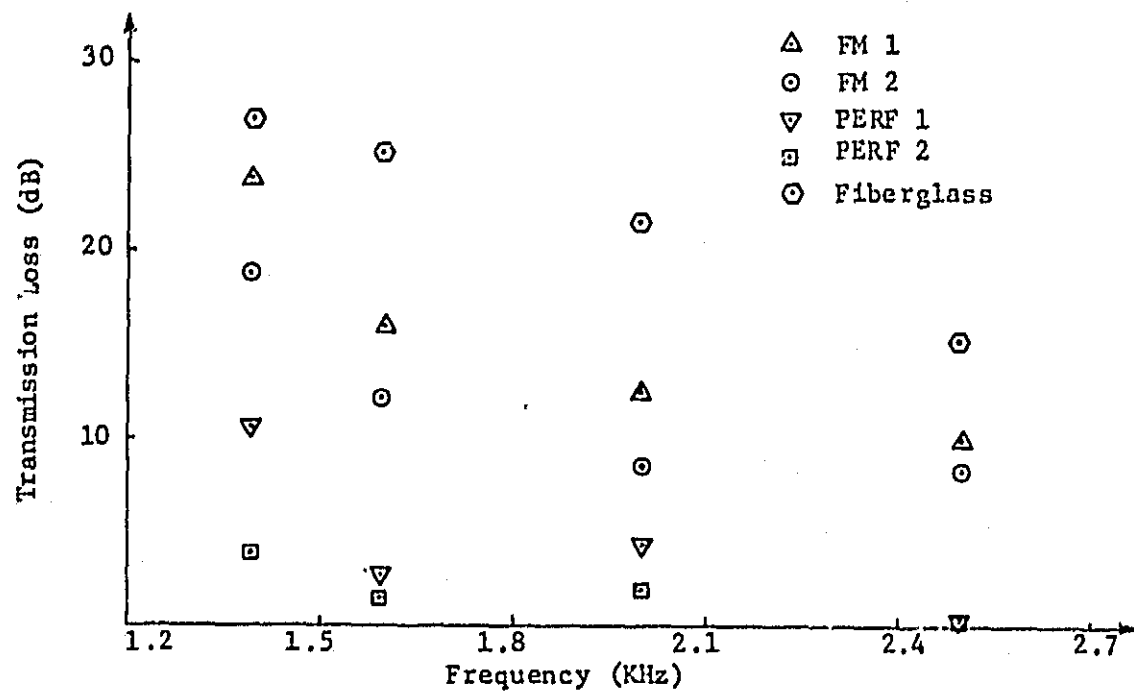


Figure 12
Transmission Loss for (0, 1)
Mode - 28-1/2" Liners

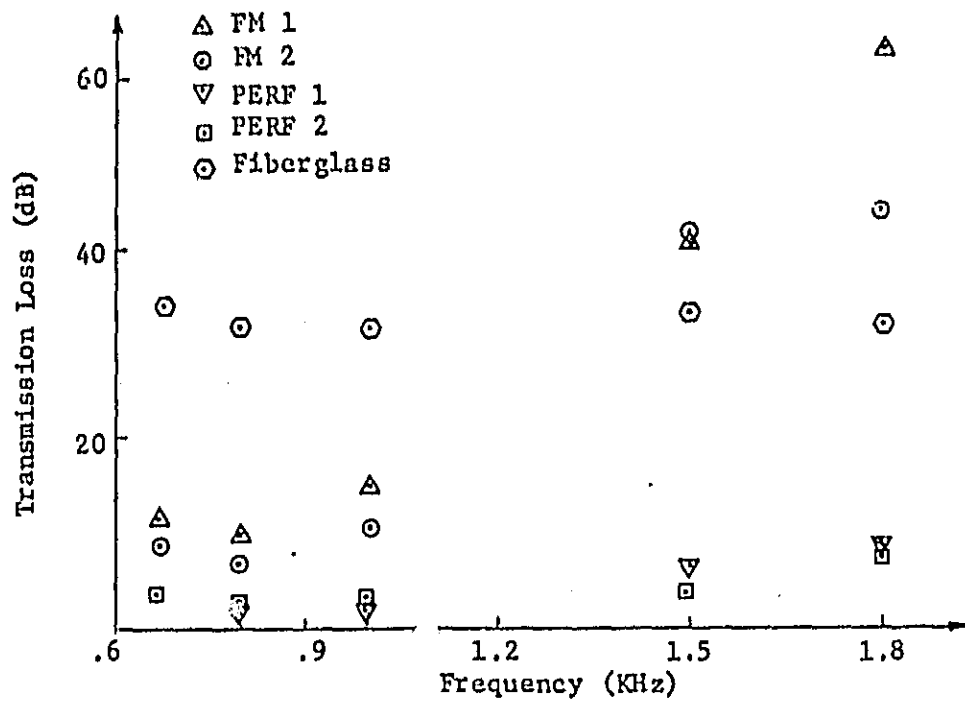


Figure 13
Transmission Loss for (1, 1)
Mode - 28-1/2" Liners

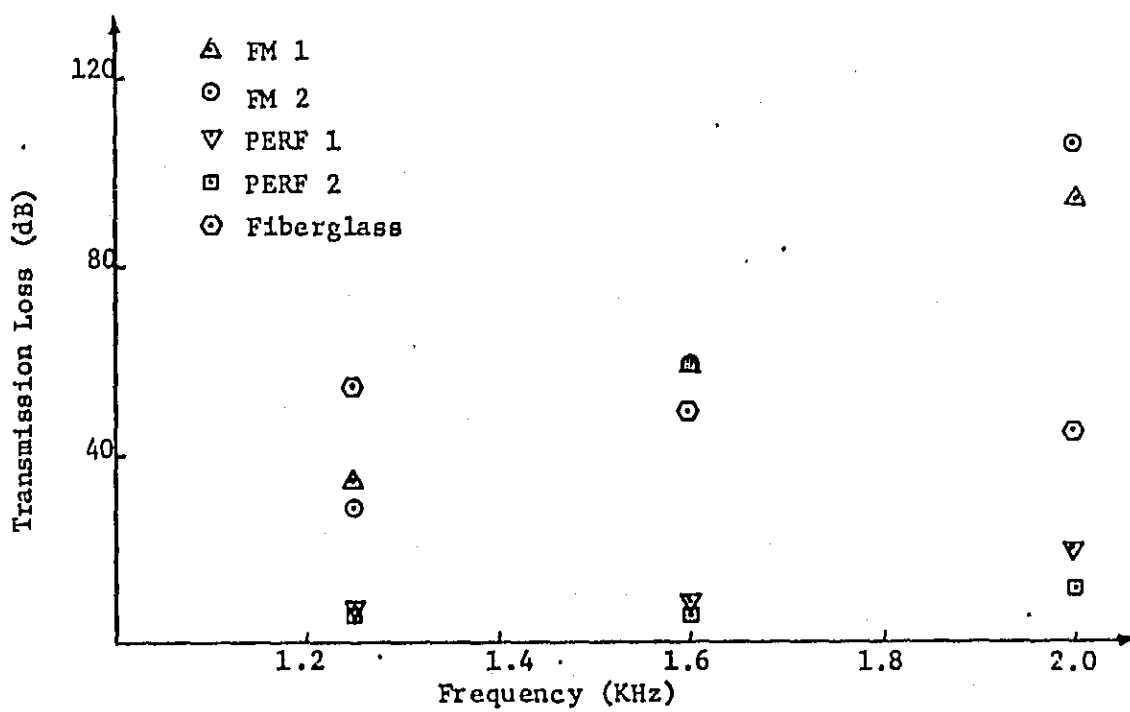


Figure 14
Transmission Loss for (2, 1)
Mode - 28-1/2" Liners